

# Utilizing Permanganate-Doped Geopolymers for Remedial Applications

Senior Thesis  
Submitted in partial fulfillment of the requirements for the  
Bachelor of Science Degree  
At The Ohio State University

By

Zachary M.K. Cotter  
The Ohio State University  
2016

*Frank W. Schwartz*

---

Franklin W. Schwartz, Advisor  
School of Earth Sciences

## TABLE OF CONTENTS

Abstract.....	ii
Acknowledgements.....	iii
List of Figures.....	iv
List of Tables.....	v
Introduction.....	1
Background.....	8
Methodology	
Materials.....	15
Sample Preparation.....	16
Column Leaching Procedure.....	18
Results	
Sample Integrity .....	19
Sample Release Characteristics.....	20
Discussion	
Sample Release .....	22
Effect of Curing and Other Factors on Sample Integrity.....	25
Conclusions.....	27
Suggestions for Future Research.....	29
References Cited.....	30
Appendix.....	32

## **ABSTRACT**

The implementation of slow release technology with in-situ chemical oxidation (ISCO) using  $\text{KMnO}_4$  has been recognized as a useful clean-up technology given its cost-effective capabilities for destroying chlorinated solvents in situ. In particular, plume treatment using slow-release technologies has been studied at The Ohio State University. This thesis focuses on geopolymers as a slow release material and aims at enhancing their slow-release performance by increasing the lifespan for permanganate release. It was hypothesized that reducing the size and degree of permanganate crystal connectivity within the matrix would increase lifetime. The investigation involved two sets of experiments: the first set of experiments termed geopolymer curing (GC) series attempted to control matrix porosity by curing at lower temperatures. The second set of experiments called the geopolymer preparation (GP) series attempted to decrease permanganate crystal connectivity by incorporating permanganate into the polymer mixture as either a concentrated solution or crushed permanganate granules. For suitable samples, 1-D column leaching experiments were conducted to observe permanganate release rates. The GC experimental series and sample GP-3 were not successful, producing distorted and soluble polymer samples. Samples prepared using crushed permanganate granules and established curing regimes produced samples ideal for analysis. Sample GP-1 was leached for 8.7 days, losing 48% of its oxidant mass, and concentrations peaking at 800 mg/L. Sample GP-2 was leached for 2.5 days, losing 28% of its oxidant mass, and concentrations peaking at 1700 mg/L. Sample GP-3 was leached for six days, losing 44% of its oxidant mass, with concentrations peaking around 850 mg/L. Sample GP-3 yielded provided the most improved rate of permanganate release. The curing schedule and duration were key to preparing a robust sample. Reducing the size of permanganate crystals before incorporation into the geopolymer enhanced the slow-release performance.

## **ACKNOWLEDGEMENTS**

I would like to thank my research advisor and mentor Dr. Frank Schwartz for all of his support, editing, advice, and great conversation. Additionally I would like to thank Dr. Anne Carey for her always appreciated guidance, input, and manuscript editing over the years. I would like to thank Dr. Utku Solpuker for his major project contributions, his hours spent teaching me, and his continued career advice. I would like to thank our funders the Global Research Laboratory (GRL), Korea project “Novel Technologies for Best Management of Non-Point Source Pollution” and the Strategic Environment Research and Development Program (SERDP) under project ER-1684. I would like to thank all of the personnel at the Subsurface Characterization and Analysis Laboratory (SEMCAL) at The Ohio State University for all of their help and permission to use their facilities. I would also like to thank my wonderful family, Dr. Berry Lyons, Dr. Thomas Darrah, Dr. Motomu Ibaraki, Dr. Gamming Liu, and all of my classmates for their support and much needed input over the years.

## LIST OF FIGURES

1. General illustration of DNAPL contamination site.....	2
2. General illustration of permanganate based ISCO scheme.....	5
3. Illustration of DNAPL remediation using slow release ISCO .....	5
4. Illustration of slow release concept.....	8
5. Illustration of polysialate-disiloxo geopolymeric structure.....	9
6. SEM image of permanganate-doped geopolymer.....	13
7. SEM Image of flushed permanganate-doped geopolymer.....	14
8. Sample GP-1 permanganate leaching trial results.....	21
9. Sample GP-2 permanganate leaching trial results.....	21
10. Sample GP-3 permanganate leaching trial results.....	22
11. Comparison plot of permanganate release rates for all samples.....	23
12. Photograph of GC-1 and GP-4 samples after curing.....	26
A1. Six Point Calibration Curve.....	32

## LIST OF TABLES

1. Chemical composition of metakoalin used in geopolymer preparation.....	15
2. Material masses used to create each geopolymer sample.....	16
3. Curing regime used to create each geopolymer sample.....	17
4. Notable molar ratios of each geopolymer sample created.....	18

## INTRODUCTION

Contamination of surface water and groundwater by organic compounds such as chlorinated ethylenes (i.e. trichloroethylene [TCE], dichloroethylene [DCE], perchloroethylene [PCE]) and polycyclic aromatic hydrocarbons (PAHs) poses a threat to human health and the environment, constituting a widespread problem at many industrial and military sites. In the 1970s and early 1980s, an ongoing effort began to identify, investigate and remediate thousands of these sites. There are some 852 sites known to be contaminated by trichloroethene alone, making it listed the 16<sup>th</sup> priority contaminant of concern (COC) within the United States according to the ATSDR priority COC list (ATSDR Priority COC List, 2016).

Many of these contaminated sites are likely to have chlorinated solvents (e.g., TCE) present as dense non-aqueous phase liquid (DNAPLs). DNAPLs pose a serious and difficult problem for remediation because of their low solubility, high density, and resistance to biodegradation. Figure 1 illustrates a conceptual model of solvent contamination at a site showing the downward flow of a DNAPL (dark red) and formation of dissolved solvent plumes. The zone of contamination near the site of leakage with DNAPL present is commonly referred to as the source area. The source area typically contains much of the mass of the contaminant. The dissolved plume can be miles and length but typically contains little of the overall mass because of the low solubility of chlorinated ethenes.

Once a DNAPL and dissolved plume have developed, it is both difficult and expensive to treat these. Early on, groundwater remediation techniques focused on plume control using methods like pump and treat. The idea with pump and treat is to keep the plume from spreading further or in some cases cleaning up the plume altogether. With pump and treat, contaminated water is pumped to the surface, treated and pumped back into the subsurface. With time however, hydrogeologists realized that there were serious issues, related to the removal



effectiveness, and life-cycle cost of this technique. During the remediation process, controlling the plume is a useful step, but because almost all of the mass is present in the DNAPL is slowly dissolving in the source area, it might take many 100s of years of operation before the site would be cleaned up. Running a pump and treat technique for hundreds of years is both expensive and impractical. Today, the pump and treat method is only considered if the source can be removed or isolated. So, several techniques need to be used together (Siegrist et al., 2011).

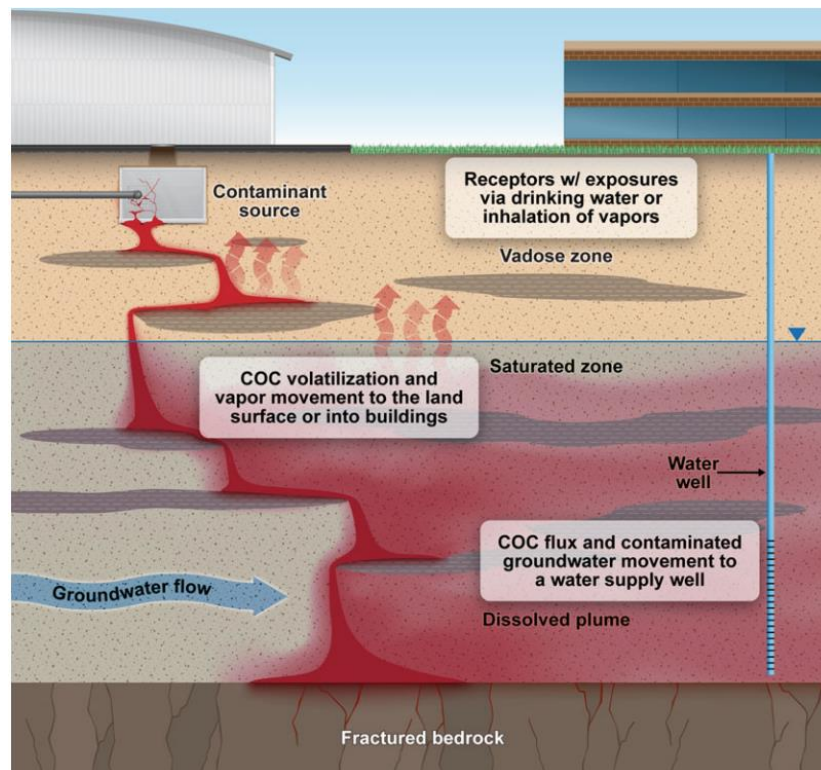


Figure 1 Illustration of a typical contamination site a source area characterized by the presence of DNAPL. Plumes of dissolved contaminants typically migrate with ambient groundwater flow (figure from Siegrist et al., 2011)

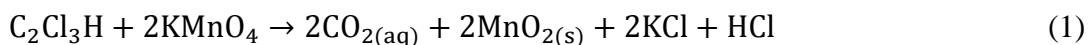
Researchers have designed remediation approaches that focus on DNAPL source areas and strategies for hydraulic plume control that are less aggressive and therefore cheaper than pump and treat. In particular, one of the newer concepts for plume control involves so called natural attenuation processes. In settings that are anoxic, natural bacterial processes are capable of destroying contaminants like TCE and PCE or similar COCs; this approach uses careful monitoring to convince regulators that the aquifer system is capable of halting plume spreading.

Natural attenuation techniques include monitored natural attenuation, aerobic cometabolism, and phytoremediation. Passive remedial technologies use reductive dechlorination, with zero valent iron walls, chemical oxidation and reduction, and electrochemical reduction to accomplish contaminant destruction when natural processes are not sufficient for complete remediation (Siegrist et al., 2011).

Students in the Schwartz Laboratory at The Ohio State University have been pioneers in basic science associated with in situ chemical oxidation (ISCO). This approach to remediation involves delivering chemical oxidants into the subsurface to destroy COCs in place. Currently, oxidants used with ISCO include hydrogen peroxide ( $\text{H}_2\text{O}_2$ ), potassium or sodium permanganate ( $\text{KMnO}_4$ ,  $\text{NaMnO}_4$ ), sodium persulfate ( $\text{Na}_2\text{S}_2\text{O}_8$ ), and ozone ( $\text{O}_3$ ). Since the 1990s ISCO using permanganate ( $\text{MnO}_4^-$ ) has been investigated and recognized as promising passive method for controlling dissolved plumes of chlorinated ethylenes (Yan and Schwartz, 1999; Zhang and Schwartz, 2000; Ibaraki and Schwartz, 2001; Li and Schwartz, 2004; Lee and Schwartz, 2007; Lee et al., 2008; Siegrist et al., 2011; Solpuker et al., 2014).

Potassium permanganate is a versatile, strong chemical oxidant favored for its relatively cheap cost, predictable chemistry, and proven ability to destroy volatile and semi-volatile organic compounds. Additionally the oxidation reaction is largely independent of pH (Siegrist et al., 2011). The oxidation reaction with permanganate transforms trichloroethene (TCE) by destroying the carbon double bonds, yielding short lived intermediates of carbon dioxide ( $\text{CO}_2$ ), manganese dioxide ( $\text{MnO}_2$ ), potassium chloride ( $\text{KCl}$ ), and hydrochloric acid ( $\text{HCl}$ ) (Eq.1) (Yan and Schwartz, 1999; Ross et al., 2005). The reaction stoichiometry, pathways, and kinetics for commonly encountered chlorinated ethane are well understood (Yan and Schwartz, 1999; Siegrist et al., 2011). Yan and Schwartz (1999) found that dissolved  $\text{KMnO}_4$  was capable of

oxidizing most chlorinated ethenes dissolved in water with half-lives ranging from 0.4 to 18 minutes. Typically, the breakdown of PCE requires much longer times with a half-life of about 4 hours. The following equation shows that oxidation by  $\text{KMnO}_4$  results in the complete oxidation of TCE to carbon dioxide, manganese dioxide and other dissolved species:



A variety of approaches is available for delivering permanganate into subsurface target zones (Siegrist, 2011). These approaches can involve the well-based injection-recirculation of dense, concentrated permanganate solutions into contaminated zones (Figure 2) or the emplacement of reactive barrier systems down-gradient of target plumes (Figure 3), (Siegrist et al., 1999, 2011; Ross et al., 2005; Lee and Schwartz, 2007; Lee et al., 2008; Solpuker et al., 2014). Other methods of permanganate delivery into target zones include injection via hydraulic fracturing, or injection into naturally fractured zones (Figure 3).

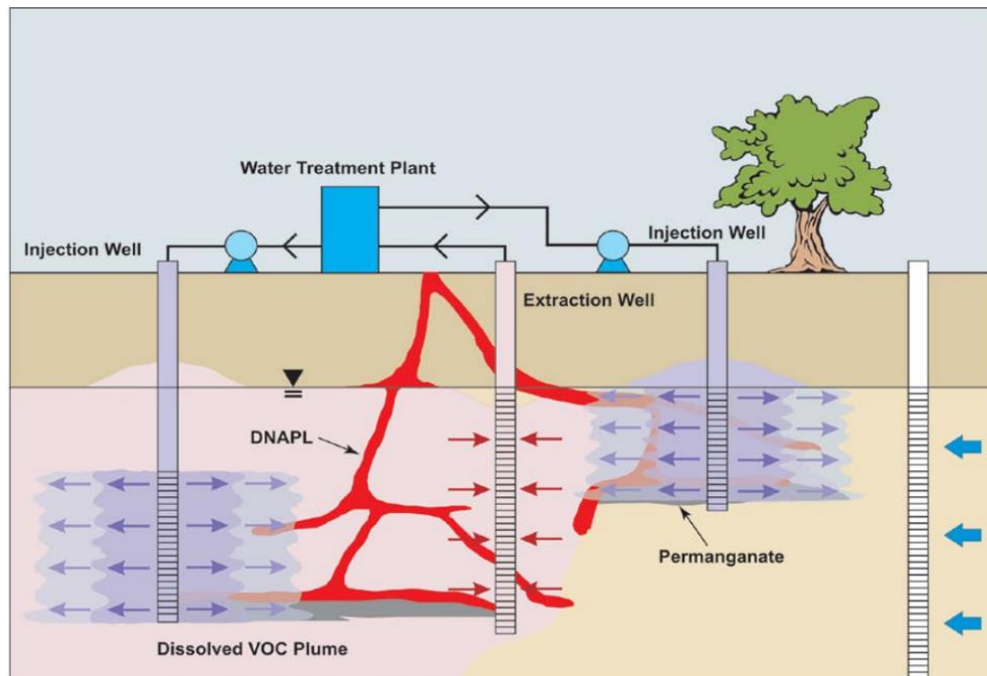


Figure 2 Schematic showing a simple injection-recirculation based ISCO treatment using  $\text{KMnO}_4$  (figure from Huling and Pivetz, 2006).

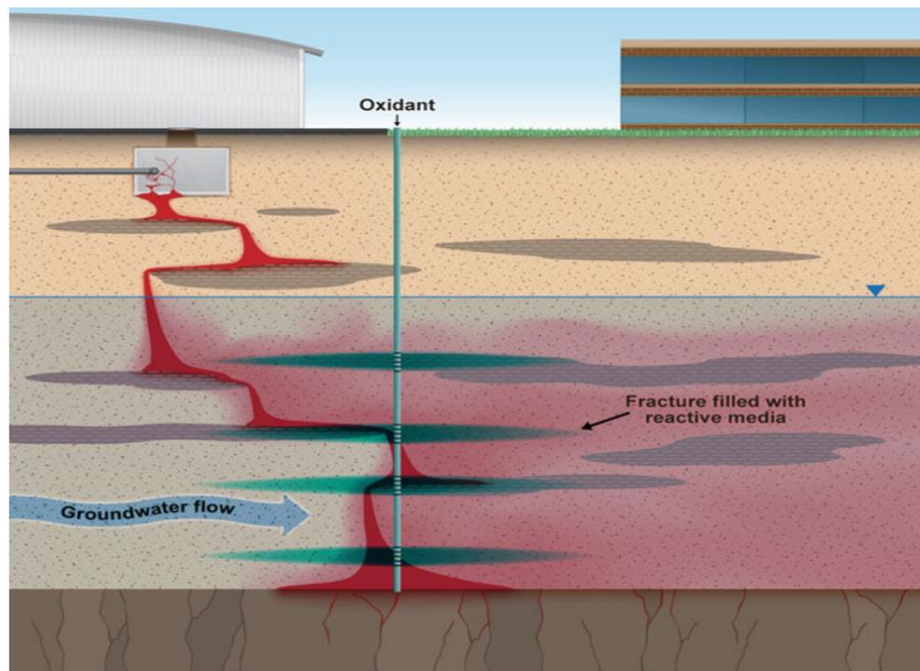


Figure 3 Illustration of DNAPL remediation using slow release barrier systems (figure from Siegrist, 2011).

Applying permanganate-based ISCO in the field is difficult; in particular, problems arise with the delivery of oxidants into target zones. One difficulty stems from complexity related to aquifer heterogeneity, particularly low permeability zones. High permeability zones tend to cause channelized flow oxidant flow, which results in poor distribution of the oxidant's mass into contaminated zones. Other problems are created by large differences in density between water with large concentrations of potassium permanganate and fresh groundwater. Density driven, mixed convection creates viscous fingering that tends to dilute oxidant concentrations. In addition, gravity underrides (due to high density of  $\text{MnO}_4$  in water) also reduces flooding efficiency with possible COC bypass, causing incomplete remediation of the COC (Ibaraki and Schwartz, 2001).

Additionally, permanganate flooding of source zones with particularly large DNAPL saturations results in pore plugging due to the precipitation of  $\text{MnO}_2$  and  $\text{CO}_2$  gas generated from the oxidation reaction. Previous studies (Li and Schwartz, 2004; Lee et al., 2008) reported a reduction in relative permeability of the medium up to 90% when large quantities  $\text{MnO}_2(\text{s})$  accumulate in pores is due to the abundance of the oxidant and dissolved permanganate in the source zone. This reduction of permeability within the medium eventually causes the oxidant flood to bypass zones with large DNAPL saturations, substantially reducing the destruction efficiency for the COC. The results is a failed remediation with large volumes of untreated DNAPL in place, increasing the probability of a rebound in aqueous concentrations once the ISCO treatment is discontinued. These problems generate the need to innovate new solutions to address the inefficiencies associated ISCO (Li and Schwartz, 2004; Lee et al., 2008).

In an attempt to address some the problems with conventional ISCO remediation schemes, several innovative strategies have been developed. One promising approach involves the

emplacement of slow-release reactive barriers downstream from the DNAPL source zone and within the dissolved contaminant plume. The reactive barrier systems creates a zone of reaction by releasing oxidants slowly within the plume to decrease the overall contaminant mobility (Ross et al., 2005; Lee and Schwartz, 2007; Lee et al, 2008; Siegrist et al 2011; Solpuker et al., 2014). The actual slow-release systems have much in common with controlled-release systems (CRS), which is used in pharmaceutical applications to extend the duration of dosing of medications.

These slow-release systems work by releasing some active treatment agent from a reservoir or matrix material (typically via diffusion) into an environment where the treatment agent is able to work to accomplish its desired task (Figure 4). CRS can be designed in such a way as to maintain a predetermined release pattern over long periods of time. In remedial settings, the idea would be to release oxidants in a prescribed manner into a plume of dissolved solvents like (TCE or DCE). The use of CRS technology in remedial systems lowers the risk of over/under dosage of the oxidant because the release characteristics are designed into the material. By targeting the plume downstream of the source zone where the oxidant requirements are minimal, the density and plugging problems are eliminated thereby reducing the possibilities of  $\text{KMnO}_4$  bypassing the COC (Lee and Schwartz, 2007). So, in effect, this provides a passive, engineering-based approach to remediation that is analogous to natural attenuation.

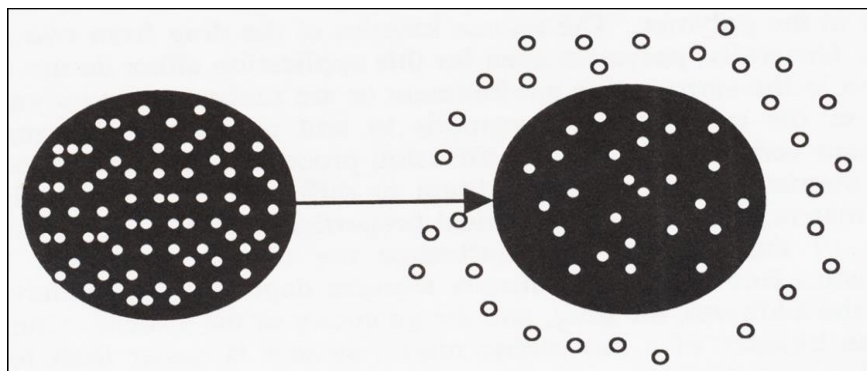


Figure 4 Illustration of controlled-release concept (Crank, 1975)

There has been a variety of slow-release solids developed for ISCO-based permanganate delivery including clay-rich slurries (Siegrist et al., 1999), oxidation resistant waxy polymers and geopolymers (Ross et al., 2005; Lee et al., 2008; Solpuker et al., 2014 ), resins (Lee and Schwartz, 2007), and stearic acid (Yuan et al., 2013). This thesis research presented herein continues the work of Solpuker et al (2014) who characterized the potential, and performance of geopolymers for subsurface permanganate delivery (Solpuker et al., 2014).

## BACKGROUND

Geopolymers have the potential to provide a novel slow release system that differs from other matrices that have been evaluated or used for permanganate delivery. Like some of these other systems, geopolymers are unreactive with permanganate and can be designed to be insoluble in water (Solpuker et al., 2014). The goal of this thesis was to study the advantages of geopolymers as a novel alternative for ISCO remediation designs. In particular, this investigation set out to determine whether oxidant-doped geopolymers represent an advance on ISCO schemes, and to identify possible ways to improve the performance of geopolymers.

Geopolymerization react aluminosilicate oxides and sodium metasilicate solution under highly alkaline conditions occurring at less than 100 °C. The reaction itself results in an

amorphous to semi-crystalline, three-dimensional silico-aluminate material (Davidovits 2002; Dimas et al., 2009). The reaction process begins with the dissolution of solid

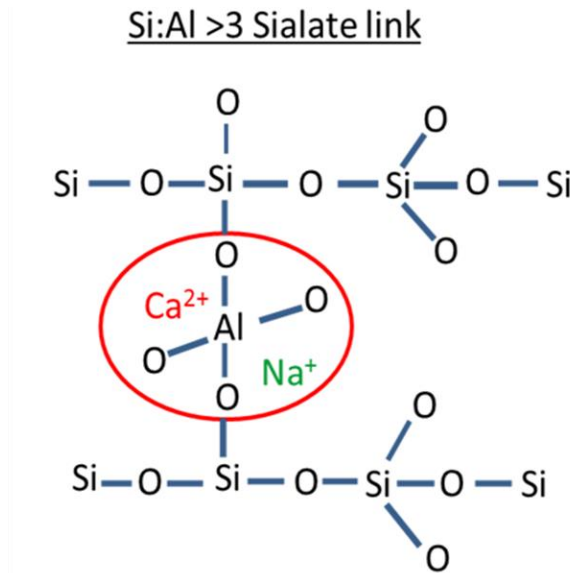


Figure 5. Illustration of atomic arrangement of a polysialate-disiloxo geopolymer (figure modified from Heah et al. 2012).

alumino-silicate materials in a strong alkaline aqueous solution (activator solution). This step results in the formation and poly-condensation of Si/Si-Al oligomers, initiating the formation of the geopolymeric framework structure. Undissolved particles are then incorporated into the final geopolymeric structure (Khale and Chaudhary, 2007; Dimas et al. 2009). The geopolymeric structure produced is a function of the molar ratio Si:Al which defines the type of geopolymer as polysialate (Si:Al=1, -Si-O-Al-O-), polysilicate-siloxo (Si:Al=2, -Si-O-Al-O-Si-O-) and polysialate-disiloxo (Si:Al=3, -Si-O-Al-O-Si-O-Si-O-) (Davidovits, 2002). In all polymer types, the three-dimensional network is composed of  $\text{SiO}_4$  and  $\text{AlO}_4$  tetrahedron linked by alternately sharing all oxygen atoms (Davidovits, 1991). Positive cations ( $\text{Na}^+$ ,  $\text{K}^+$ ,  $\text{Li}^+$ ,  $\text{Ca}^+$ , etc.) act as charge balancing agents for the net negative charge created by  $\text{AlO}_4$  (Davidovits, 1991).



The rate at which the geopolymerization reaction occurs is influenced by curing temperature, activator solution concentration, mass of initial solids, chemical composition, and the type of source material (Rowles and O’Conner, 2003; Criado and Jimenez, 2007; Kong et al., 2007; Dimas et al., 2009). A study conducted by Rowles and O’Conner (2003) found that compressive strength is maximized when there is a slight excess of Na concentration compared to the assumed Na:Al molar ratio needed for charge balancing, and when the Si:Al molar ratio is approximately 2.5. Furthermore, the solubility of the geopolymer decreases as  $\text{SiO}_2/\text{Na}_2\text{O}$  ratios increase, and when Si/Al ratios are below five, the geopolymer is practically insoluble (Dimas et al., 2009).

Solpuker and others (2014) characterized the release rates and mass transport of several permanganate-doped geopolymers. In practice, permanganate was added to the geopolymer as crushed crystals during one of the last mixing steps in creating the polymer-mix. Because small quantities of water are present in the mix, some of the crystalline permanganate salt dissolves in the water. Later, as the geopolymer is cured, the water evaporates and the dissolved permanganate re-precipitates as small crystals. Not surprisingly, imaging with a scanning electron microscope (SEM) found samples composed of a  $\text{KMnO}_4$ -doped ground matrix with larger interclasts of undissolved permanganate solids (Figures 6 and 7).

These geopolymers release the embedded permanganate through dissolution from the outside of the sample into the interior. Although  $\text{KMnO}_4$  crystals dissolve quickly in water, the release of permanganate becomes diffusion-controlled because dissolved mass need to be transported out of the geopolymer before additional dissolution can occur. Solpuker et al. (2014) characterized the mass transport occurring when the permanganate doped geopolymers were

leached. The quantity of permanganate released through time was modelled according to a Fickian-based drug delivery model, governed by equation 2 below,

$$M_t/M_\infty = kt^n \quad (2)$$

where  $M_t$  and  $M_\infty$  are the cumulative amount of drug released at times  $t$  and infinity (release completed),  $k$  is the kinetic constant,  $n$  is the release exponent, and  $t^n$  is characteristic of the chemical/polymer-system. Equation 2 is only valid until the fractional release of the chemical is  $< 0.6$ , where the assumption of perfect sink conditions is valid (Peppas 1985; Ritger and Peppas 1987; Solpuker et al., 2014).

Modeling leads naturally to a way of classifying the type of transport operating to move mass out of the polymer matrix. With a Case I system, release is primarily diffusion controlled with a constant diffusional constant indicated when  $n = 0.45$ . With a Case II system, other processes besides diffusion are operative and are indicated by a larger  $n$  value (i.e.,  $1 > n > 0.45$ ). Case II system transport thus provide faster (and cumulatively larger) releases of the active agent as compared to diffusion alone. Classical theory explains Case II as a relaxation effect where the polymeric structure of the matrix opens up enhancing transport through time. My system is different in that the structure is opening up because  $\text{KMnO}_4$  is gradually dissolving not relaxing. Qualitatively, although these processes are different, the net effect is the same and equation 2 still applies (Crank, 1975; Frisch, 1980; Solpuker et. al, 2014).

Solpuker et al (2014) found that the permanganate doped geopolymers released oxidants through several process, providing a complex pattern of oxidant loading. All geopolymer samples with varying permanganate densities exhibited  $n$  values greater than 0.45. As more permanganate was packed into a given sample of geopolymer, the  $n$  values became higher. This result suggests that within the doped-geopolymer systems, releases increasingly deviate from

Fickian-diffusional behavior as the quantity of added  $\text{KMnO}_4$  was increased. Solpuker et al. (2014) attributed these increasing permanganate release rates to secondary porosity produced by the dissolution of  $\text{KMnO}_4$  within the matrix and pore spaces, creating macro-pore pathways for additional water to penetrate the CRS. Samples with higher permanganate concentrations were governed more strongly by Case II transport than Case I transport. Because of the higher release rates for the more concentrated samples, they exhibited a shorter lifetime than the less concentrated samples (Solpuker et al., 2014).

This investigation attempts address the potential of increasing the permanganate-doped geopolymer lifespan by attempting to control the size and degree of permanganate crystal connectivity within the matrix. The first experiment set (GC series) attempted to control matrix porosity by curing at lower temperature regimes. Samples GC-1 and GC-2 were prepared with identical preparation methods but were cured at different temperatures for different durations. The second experiment set (GP-3) attempted to decrease permanganate crystal connectivity by incorporating permanganate into the geopolymer paste as either a solution or as crushed permanganate granules (crushed with mortar and pestle).

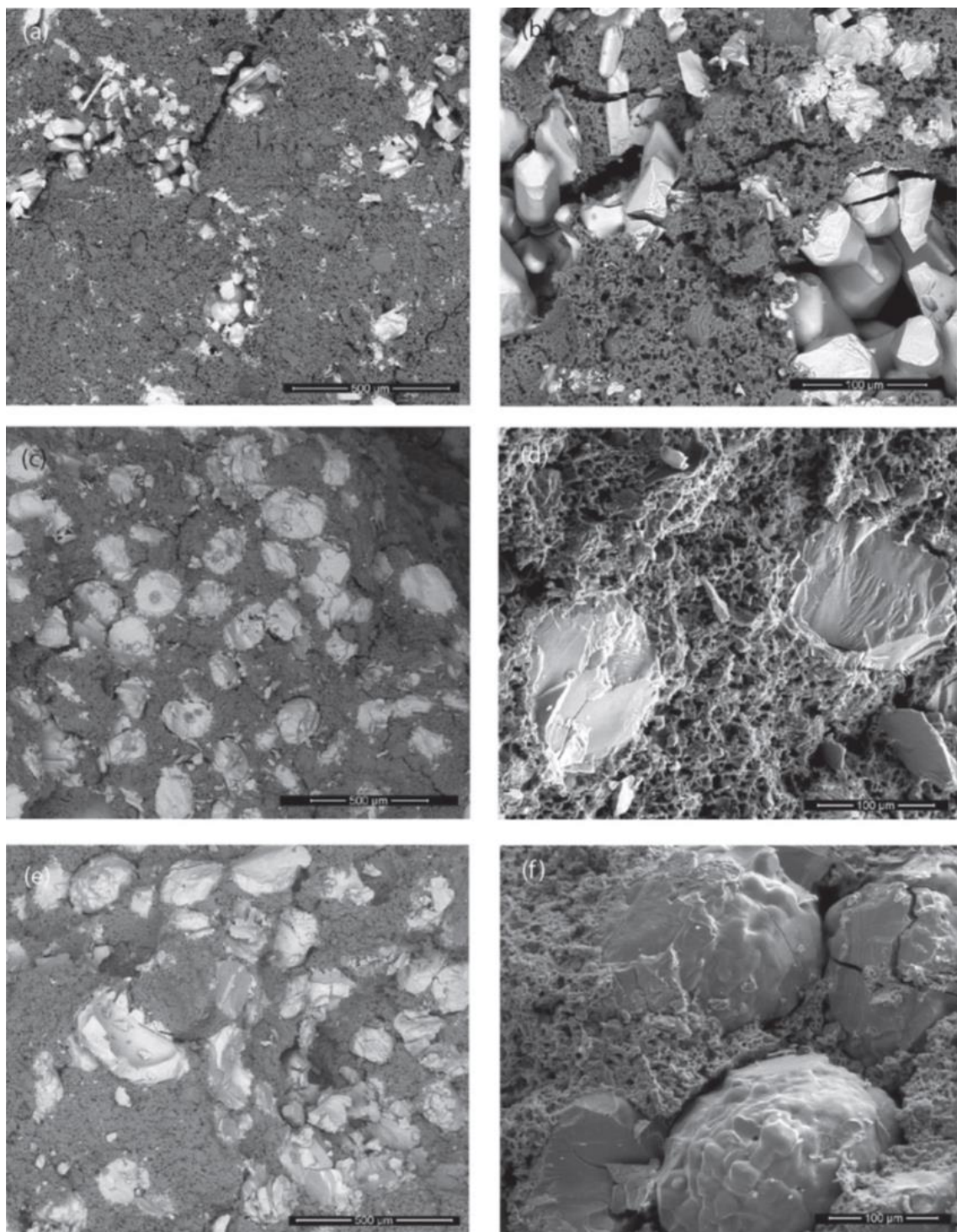


Figure 6. Images of permanganate-doped geopolymers. Image A and B feature a permanganate density of  $1.40 \times 10^{-1} \text{ g/cm}^{-1}$ . Images C and D feature a permanganate density of  $4.63 \times 10^{-1} \text{ g/cm}^{-1}$ . Images E and F feature a permanganate density of  $6.07 \times 10^{-1} \text{ g/cm}^{-1}$  (images from Solpuker et al., 2014).



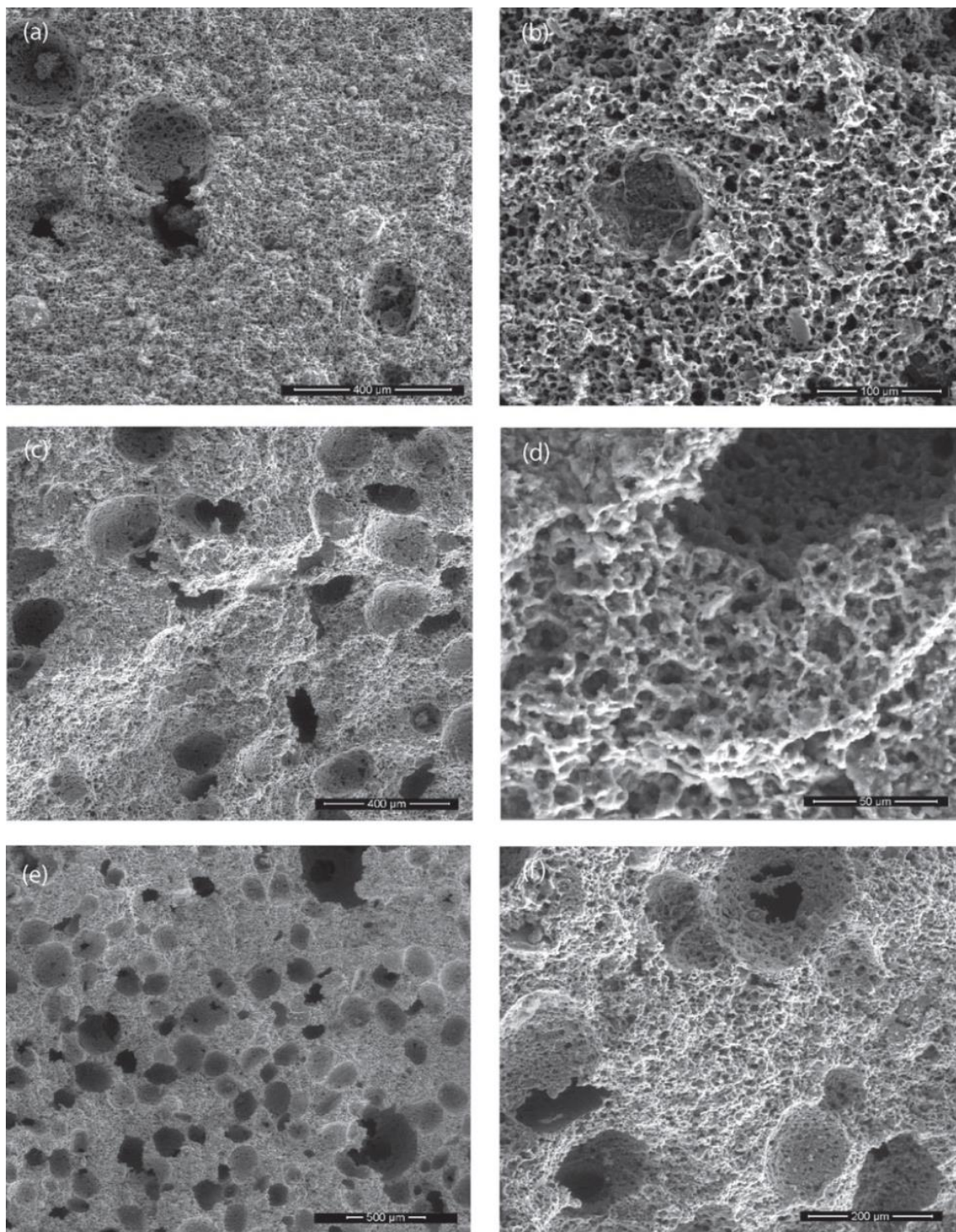


Figure 7. SEM images of permanganate doped geopolymers after column leaching experiments. Images A and B feature a permanganate density of  $1.40 \times 10^{-1} \text{ g/cm}^{-1}$ . Images C and D feature a permanganate density of  $4.63 \times 10^{-1} \text{ g/cm}^{-1}$ . Images E and F feature a permanganate density of  $6.07 \times 10^{-1} \text{ g/cm}^{-1}$  (images from Solpuker et al., 2014).

## METHODOLOGY

### Materials

The geopolymer created for this study required several components. Refined, dehydroxylated metakaolin (PowerPozz white) was purchased from Advanced Cement Technologies Company (Blaine, Washington). Metakaolin is produced by calcination of purified kaolin. It is this highly reactive material that provides the cement-like characteristics when used as an additive for a geopolymer. The composition of the metakaolin was identified via XRD analysis and is summarized in Table 1. As expected,  $\text{SiO}_2$  and  $\text{Al}_2\text{O}_3$  are the major constituents. The metakaolin has a density of  $2.6 \text{ g/cm}^3$ , a particle size distribution of 2–25  $\mu\text{m}$ , and a specific surface area of  $15 \text{ m}^2/\text{g}$  (Solpuker et al., 2014). In order to promote polymerization, an additional silicate source was provided in the way of “N-Clear” Sodium silicate solution ( $\text{Na}_2\text{SiO}_3$ ), purchased from PQ Corporation (Malvern, PA). The N-Clear solution has 37.5 weight percent of solids and exhibits a  $\text{SiO}_2/\text{Na}_2\text{O}$  weight ratio of 3.22. The pH, density, and viscosity of the sodium metasilicate solution were 11.3,  $1.39 \text{ g/cm}^3$ , and 180 centipose at  $20^\circ\text{C}$ . The alkali-activator for geopolymerization was NaOH pellets (98.5% purity) purchased from Acros Organics located in Bridgewater, NJ. Potassium permanganate granules (Cairox-Cr) added to the geopolymer was purchased from Carus Corporation located in LaSalle, Illinois.

Table 1. Chemical composition of metakaolin used in study, analyzed via x-ray diffraction (from Advanced Cement Technologies, 2013)

Abundance of Key Constituents (%)										
$\text{SiO}_2$	$\text{TiO}_2$	$\text{Al}_2\text{O}_3$	$\text{Fe}_2\text{O}_3$	$\text{MgO}$	$\text{CaO}$	$\text{Na}_2\text{O}$	$\text{K}_2\text{O}$	$\text{SO}_4$	$\text{P}_2\text{O}_5$	LOI
51-53	<3.0	42-44	<2.2	<0.1	<0.2	<0.05	<0.4	<0.5	<0.2	<0.5

### Sample Preparation

Five permanganate-doped geopolymer samples were prepared, each with variations in preparation or in the manner of incorporation of  $\text{KMnO}_4$  into the geopolymer structure. The general preparation of each geopolymer sample was initiated by dissolving sodium hydroxide pellets into a sodium silicate solution. The solution was mixed by hand until the NaOH pellets were fully dissolved, creating a highly alkaline solution (activator solution), initiating the Si/Si-Al oligomerization process. Metakaolin was next added into the solution to serve as an additional alumino-silicate source. As before, manually mixing continued until the metakaolin fully dissolved. Lastly, permanganate (solution or granules) was then added into the solution and mixed manually. Table 2 shows the masses used of each component used to create individual samples. Once the doped geopolymer paste was prepared, it was poured into cylindrical molds and tapped against a hard surface until all of the air bubbles were eliminated.

Table 2. Material masses used to create each geopolymer sample.

<b>Material</b>	<b>GC-1</b>	<b>GP-1</b>	<b>GP-2</b>	<b>GP-3</b>	<b>GP-4</b>
<b>Sodium silicate (N-Sil) (g)</b>	210	105.00	70.0	105.0	70.0
<b>Metakaolin (g)</b>	90	45.00	30.0	45.0	30.20
<b>NaOH (g)</b>	4.5	2.25	1.50	2.25	1.50
<b>KMnO<sub>4</sub> (g)</b>	30.2	10.00	9.20	10.0	10.0
<b>H<sub>2</sub>O (ml)</b>	-	-	-	-	15.0

The preparation method varied somewhat with the goal of understanding how preparation might influence the behavior of the control-release materials. The GC series of samples featured variations among curing regimes. The GP series of samples tested the ability to decrease permanganate crystal connectivity and size within the geopolymer matrix by varying the manner in which permanganate was incorporated into the geopolymeric structure. The GP series of

experiments consisted of three samples featuring crushed permanganate granules (using a mortar and pestle) or a highly concentrated permanganate solution. Tables 3 and 4 displays the curing regime and notable molar ratios for each geopolymer sample created for the study.

Table 3. Curing regime used to create each geopolymer sample.

<b>Sample</b>	<b>Curing Temperature (<math>^{\circ}\text{C}</math>)</b>	<b>Curing Duration (hr)</b>	<b>Vaccum (Torr)</b>
<b>GC-1</b>	<b>40</b>	<b>24</b>	<b>350</b>
<b>GP-1</b>	<b>75</b>	<b>48</b>	<b>350</b>
<b>Gp-2</b>	<b>23</b>	<b>24</b>	<b>350</b>
	<b>40</b>	<b>24</b>	
	<b>23</b>	<b>72</b>	
<b>GP-3</b>	<b>75</b>	<b>48</b>	<b>350</b>
<b>GP-4</b>	<b>80</b>	<b>48</b>	<b>350</b>

The preparation method was problematic due to inadequate mixing and curing utilities available; some of the samples that were produced were not suitable for further testing. For example, samples ended up cracking during preparation or expanding or expanding out of the casting cylinder. When obviously flawed, the samples were discarded.

Table 4. Molar ratios of each geopolymer sample prepared.

<b>Sample</b>	<b>Si/(Na+K)</b>	<b>Si/Al</b>	<b>(Na+K)/Al</b>
<b>GC-1</b>	<b>1.58</b>	<b>2.74</b>	<b>1.73</b>
<b>GP-1</b>	<b>2.09</b>	<b>2.35</b>	<b>1.12</b>
<b>GP-2</b>	<b>2.4</b>	<b>2.35</b>	<b>0.98</b>
<b>GP-3</b>	<b>2.09</b>	<b>2.35</b>	<b>1.12</b>
<b>GP-4</b>	<b>1.93</b>	<b>2.35</b>	<b>1.21</b>

### Column Leaching Apparatus and Procedure

1D column leaching experiments were conducted in order to observe variations of permanganate-mass release through time of samples that qualified for further experimentation. The leaching columns were made from glass (Kontes Chromaflex,) with an inner diameter of 4.8 cm and a length of 5.1-5.6 cm.



An experiment was run by placing the geopolymer in the glass column and flowing RO (reverse osmosis) water through the column. Specialized end-caps both provide tubing connections for inflow and outflow from the column and distributed the inflows and outflows across the entire area of the column. Ambient flow of RO water was provided using Ismatec Ecoline peristaltic pumps in order to provide “perfect sink conditions” meaning that permanganate concentration in the column in the fluid surrounding the sample is negligible at all times (Seipmann et al., 2012).

Concentration of dissolved permanganate ( $\text{MnO}_4^-$ ) in water flowing out of the column was measured continuously using a flow-through cell on an ultraviolet-visible (UV-Vis) spectrophotometer (Shimadzu UVmini-1240). Sample readings were taken every minute and read at a wavelength of 525 nm. At the beginning of the experiment, samples were taken manually, diluted, and then placed into the UV-Vis instrument in order to accommodate samples outside of the operating concentration range of the instrument. Once initial high  $\text{MnO}_4^-$  concentrations declined, automatic sampling analysis by the UV-Vis instrument was then initiated via the flow-through cell.  $\text{MnO}_4^-$  concentration was calculated from absorbance based on a six-point calibration curve (see figure A1 in the appendix).

## **RESULTS**

The results describe two features of the overall sample performance as a slow release system. Sample integrity turned out to be an important feature of the overall behavior. This researcher had problems in producing testable samples. Some samples cracked to the extent that major segments fell off. In assessing curing as a controlling feature, my study herein some cases necessarily deviated from the approach of Solpuker et al. (2014) that produced competent samples on a consistent basis.

The second feature of each sample that is reported here is the release rate of permanganate. The emphasis here is trying to use geopolymers to improve on the slow release materials discussed in the introduction.

### **Sample Integrity**

Sample GC-1 was produced using a rapid curing method. The result was a distorted and poorly polymerized sample that lacked the characteristic insolubility of our previous geopolymers (Solpuker et al., 2014). Because of its distorted shape and solubility, no column flow testing was conducted on the sample. It is likely that the sample simply failed to polymerize because inadequate curing.

The GP series of experiments produced predictable samples that were insoluble. Sample GP-1 featured the standard permanganate granule size and was cured using a standard curing regime (Solpuker et al., 2014), yielding a strong and insoluble sample. Sample GP-2 and GP-3 both featured much more finely crushed permanganate granules. In addition, sample GP-2 featured a prolonged curing regime. Sample GP-3 differed from Sample GP-1 only in terms of the finer crushing of the  $\text{KMnO}_4$  crystals. Both curing techniques produced insoluble, strong samples; both were subjected to column tests for performance analysis.

Sample G-4 resulted from an attempt to load up the sample with more  $\text{KMnO}_4$  by incorporating a highly concentrated permanganate solution into the geopolymer paste instead of solid permanganate granules. After mixing the permanganate solution into the geopolymer paste, the viscosity quickly diminished and the mixture lost cohesion. After curing, the GP-4 sample proved to be soluble, weak, and distorted; no performance testing was conducted.

### **Sample Release Characteristics**

A series of simple column flow experiments were conducted for samples GP-1, GP-2, and GP-3. For each sample, the concentration of  $\text{MnO}_4^-$  in the column effluent is plotted versus time (Figures 8, 9, 10). Additionally the cumulative release of permanganate is shown as the percentage of mass released to the total quantity of  $\text{KMnO}_4$  originally present in the sample (Figures 8, 9, 10). Sample GP-1 was leached for 8.7 days, losing 48% of its oxidant mass, and concentrations peaking at 800 mg/L (Figure 8). Sample GP-2 was leached for 2.5 days, losing 28% of its oxidant mass, and concentrations peaking at 1700 mg/L (Figure 9). Sample GP-3 was leached for six days, losing 44% of its oxidant mass, with concentrations peaking around 850 mg/L (Figure 10). Generally, the release behaviors of all samples were similar. The largest concentrations of  $\text{KMnO}_4$  were evident at early times. Concentrations declined exponentially reflecting the transition to a diffusion controlled releases. Samples GP-1 and GP-3 were only slightly different from each other in terms of release behavior. Sample 2 was much different with initially much higher early concentrations followed by much smaller concentrations later.

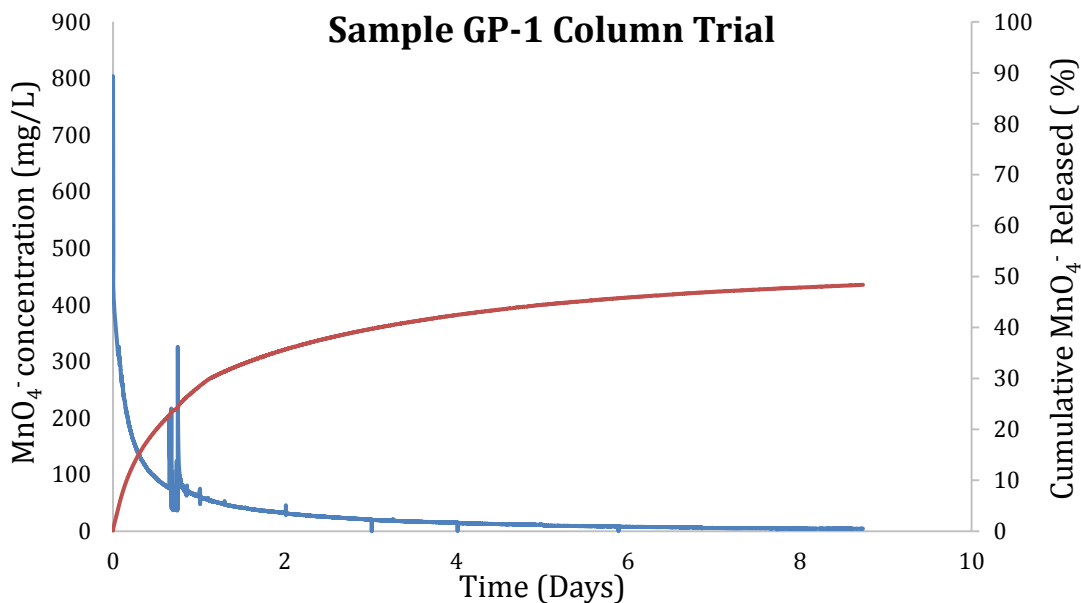
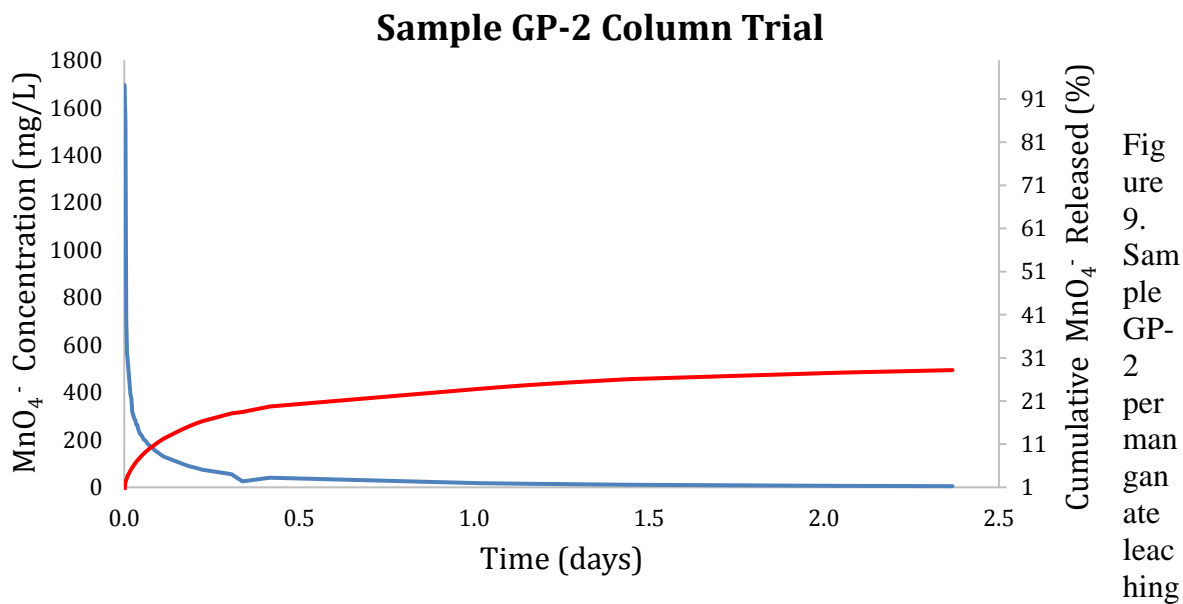


Figure 8. Sample GP-1 permanganate leaching trial results. The left axis is permanganate concentration (shown in blue). The right axis is the cumulative release of permanganate (shown in red). The bottom axis is time.



trial results. The left axis is permanganate concentration (shown in blue). The right axis is the cumulative release of permanganate (shown in red). The bottom axis is time.

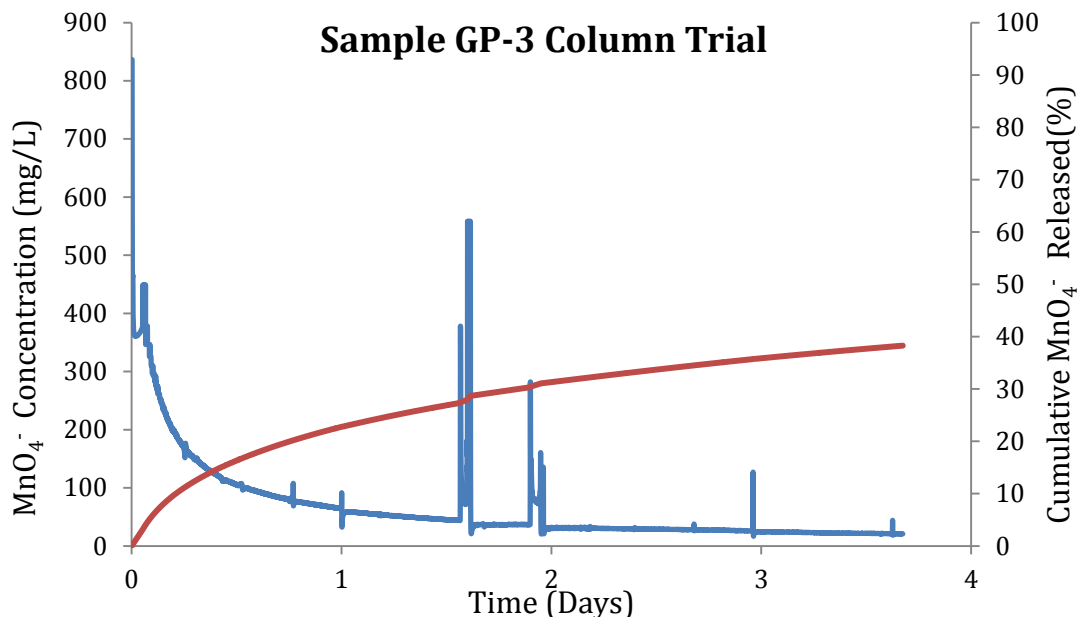


Figure 10. Sample GP-3 permanganate leaching trial results. The left axis is permanganate concentration (shown in blue). The right axis is the cumulative release of permanganate (shown in red). The bottom axis is time.

## DISCUSSION

There are two essential features of the overall sample performance as a slow release system. The first is the rate at which permanganate is released for each sample, especially in relation to each other. Thus, following here is a discussion of how release rates of individual samples subjected to column flow testing compared to each as a basis for evaluating how the various adaptations of the doped-geopolymers affect slow-release performance. A second aspect of the discussion focuses on the effect of curing on sample integrity. As stated previously, sample integrity proved to be an important feature in controlling the slow-release properties of each sample.

### Sample Release Performance

Samples GP-1, GP-2, and GP-3 were subjected to column flow testing for various time periods. Sample GP-1 was a stock sample, prepared identically to the proven methods from our

previous study (Solpuker et al., 2014). Sample GP-2 was prepared with crushed permanganate granules and an extended curing schedule. Finally, the last sample GP-3 was prepared with crushed permanganate instead of stock industrial permanganate crystal size (sample 1), utilizing an identical curing schedule to sample GP-1. The permanganate release functions for each sample are displayed together in Figure 11 below. The concentration of released permanganate (mg/L) in the column effluent is shown by a solid blue line with its cumulative permanganate release (%) shown in dashed blue. The permanganate concentration in the column effluent for

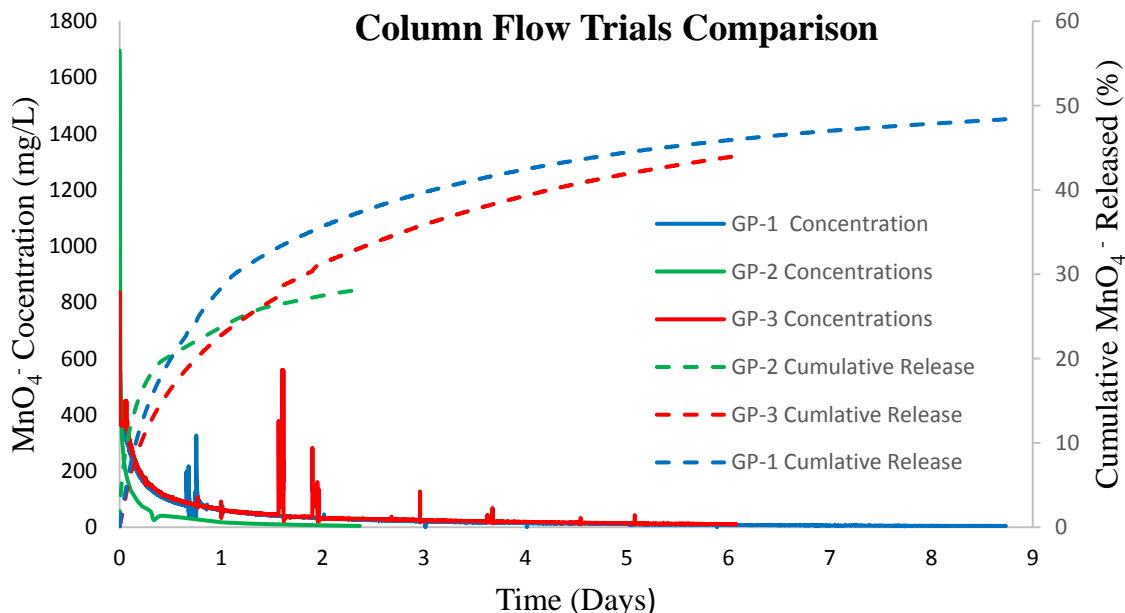


Figure 11. A comparison plot of permanganate mass released from all samples during column flow experiments. As explained in the text, the solid, colored lines show permanganate concentrations in the column effluent. The dashed lines show the cumulative release behavior. sample GP-2's (mg/L) is shown in solid green with cumulative release (%) indicated by a dashed green line. Comparable results are presented for sample GP-3 with solid red and dashed red lines.

Sample GP-1 (stock sample), as expected, produced comparable rates of permanganate release as the samples from our previous study (Solpuker et al., 2014). Preliminary indications

with sample GP-2 (crushed permanganate granules and a prolonged curing schedule) are that changes to the curing schedule could enhance the slow-release behavior. Initially, permanganate concentrations in the column effluent were higher than other samples ( $\sim 2\times$ ). Subsequently, however, release rates were apparently much lower than observed with the other two samples. Moreover, the release rate for GP-2 became even slower with time.

These results are however somewhat equivocal for several reasons. First, sample GP-1 and GP-3 in which permanganate concentrations were recorded every minute automatically, sample GP-2 fell outside the upper limit for automatic measurements by the UV-Vis. Consequently, samples were collected and measurements were made manually sometimes with hours rather than minutes between measurements. This inadequate sampling makes the assumption that permanganate release is constant between sampling intervals, which is most likely invalid. Second, the initial rapid release followed by a sharp decline is characteristic of flow from a fractured medium. Without SEM analysis to verify the absence of fractures within sample GP-2, so no valid conclusions can be made about the effect that the prolonged curing schedule had on sample performance.

Sample GP-3 yielded the best improvement in reducing the rate of permanganate release. Permanganate concentrations in the column effluent for sample GP-3 initially started out about the same as GP-1 but quickly tracked below sample GP-1 over time (Figure 11). Similarly, at comparable times, the cumulative release rates for sample GP-3 was lower than that of GP-1 indicating that more mass was present in GP-3 throughout the test. With the curing schedules, permanganate density, sampling methods and mathematical analysis between sample GP-1 and GP-3 being identical, it plausible that crushing permanganate granules before addition into the geopolymer paste had a positive effect on increasing the slow-release lifetime of sample GP-3.

The crushing of permanganate granules most likely decreased the permanganate crystal size and reduced the pore size and connectivity within the final cured sample. This would make it more difficult for water to enter the sample and for permanganate to diffuse out. This conclusion makes sense in the context of our previous work. However, this it would need to be verified with SEM analysis of the leached sample, which was beyond the scope of the present investigation.

### **Effect of Curing and Other Factors on Sample Integrity**

Sample GC-1 was produced under rapid curing conditions, resulting in a distorted, soluble and poorly polymerized specimen compared to the more robust samples from our previous work (Solpuker et al., 2014). The sample GC-1 mixture was cured in was open-ended steel cylindrical mold, which probably caused the poor outcome. The cylinder is essentially an open-curing system in which the relative humidity and dehydration rate was uncontrolled.

Sample GP-4 also failed to produce a slightly different form of slow-release system. The idea tested with this sample was to add  $\text{KMnO}_4$  not as particulate solid granules but as a concentrated permanganate solution. As curing occurred and the water was driven off, the dissolved permanganate should precipitate as smaller crystals. It was hypothesized that overall as these  $\text{KMnO}_4$  crystals would allow for broader dissemination of the permanganate in the sample and much slower release rates. This sample was cured using methods proven by Solpuker et al. (2014) with one exception. Sample GP-4 was cured in a plastic Nalgene screw-top bottle, in which the cap was loosely sealed (to control humidity of environment). Upon curing, sample GP-4 appeared very similar to sample GC-1.

The samples produced were deformed in such a way as to suggest the mixture was in a boiled state, so much that the mixture rose above the extent of the curing molds (Figure 12). Both



samples appear to have vesicles, where water vapor was expelled from the boiling polymer mixture.

Lizcano et al. (2012) stated that once the geopolymerization reaction is initiated and before completion of the curing stage, water molecules often sit between the silicate links of the



Figure 12. Photograph of the GC-1 and GP-4 series of samples after curing.

geopolymer structure. Once curing begins, water evaporates from the mixture, leaving a condensed hardened structure. The rate of dehydration and the relative humidity of the curing environment are the most important factors controlling the integrity of the polymer. In the case of GC-1, it is likely that the open-ended character of steel mold caused the sample to experience rapid dehydration leading to the distorted samples (Figure 12).

Sample GP-4 was cured in a much more controlled environment; however sample GP-4 had much more water present within the mixture as a result from using a permanganate solution. Sample GP-4 most likely became dehydrated too quickly or experienced a reduction in mass so much that the result was a highly disorganized polymer. As stated previously, sample GP-2 was subjected to a prolonged curing schedule at lower temperatures, and produced apparent positive results. However, with the exception of producing an insoluble and modestly robust sample, the

effect the curing had on its slow-release performance cannot be validated as a result of limited experimentation and poor sampling methods throughout the study.

This research has shown that slow release systems using geopolymers are difficult to prepare. Considerably more work and a much more sophisticated production system are required to prepare high quality samples on a consistent basis compared with previous approaches used in our laboratory, where mixing permanganate with melted wax or in organic resins provided slow-release solids and that can be prepared in much more basic laboratory settings.

## **CONCLUSIONS**

Slow release geopolymer systems have potential as in-situ chemical oxidation schemes for the delivery of chemical oxidants within the subsurface. Investigations of utilizing geopolymers for slow-release applications have continued to yield promising results. The effect of curing environment and duration was proven to be strong influence in the preparing a robust sample and potentially has a positive effect on the slow-release performance. The addition of permanganate in a dissolved state into geopolymer mixtures produces poor quality samples and most likely has low potential of being an improvement to the control-release configuration. The crushing of solid permanganate crystals before incorporation into the geopolymer mixture has an apparent positive effect on the slow-release performance of the doped-geopolymers.

The geopolymer family of slow release systems has potential for increasing the duration of releases. However, as this study showed, making these materials is complex and will require considerably more testing before geopolymers will successfully compete with simpler material schemes (waxes and resins). One major obstacle facing anyone who aims at further developing controlled-release geopolymer systems is the inability to consistently produce identical samples with desired properties (solubility, compressive strength etc.). The process of polymerization is

extremely sensitive to changes in curing environment and composition. Factors such as relative humidity, pressure, starting material composition, and temperature were shown to be important in determining the geopolymeric structure, porosity, compressive strength, solubility, and most likely their mass-release capabilities.

## **RECOMMENDATIONS FOR FUTURE WORK**

Unfortunately, the geopolymer family of slow release systems is not yet competitive with simpler schemes already developed (wax or polymer matrices). Additional work is required using more advanced approaches that provide more precise control over factors such as mixing, curing temperature, and humidity. Control of these factors would require a dedicated high end laboratory with appropriate ovens and casting systems. Preparation of geopolymer samples by hand lead to heterogeneous polymers. The most critical needs are automated mixers and advanced curing ovens are needed to ensure that all materials are dissolved, consumed within the reaction, and evenly distributed within the geopolymeric structure. These changes would facilitate a much more systematic preparation method leading a much more consistent set of good samples needed for properly comparing performance characteristics potential of slow-release geopolymers.

Additionally, to properly examine the effect various preparation methods (such as the variations examined by this study) have on slow-release potential, more rigorous investigations of the samples, especially characterization of porosity and permeability, in addition to mass transport rates is required. These data could be interpreted to show exactly how these parameters influence release rates and potential processes that could be available for system optimization. Possible methods to examine effects on porosity include SEM imaging using a point counting method to estimate the porosity or gas absorption to estimate porosity and permeability. Estimates of permeability and diffusion rates could be done using inverse-based model approaches.

## REFERENCES CITED

- Advanced Cement Technologies, 2013, Metakaolin physical and chemical properties-standard: <http://www.metakaolin.com> (accessed May, 2016).
- ATSDR Priority COC list, retrieved June 18, 2016 from <https://www.atsdr.cdc.gov/spl/>
- Crank, J., 1975, *The Mathematics of Diffusion*, Great Britain, Oxford University Press.
- Criado, M., and Fernandez-Jimenez, A., 2007, An XRD study of the effect of the SiO<sub>2</sub>/Na<sub>2</sub>O ratio on the alkali activation of fly ash: *Cement and Concrete Research*, v.37, no.5, p.671-679, [doi:10.1016/j.cemconres.2007.01.013](https://doi.org/10.1016/j.cemconres.2007.01.013)
- Davidovits, J., 1991, Geopolymers: Inorganic polymeric new materials: *Journal of Thermal Analysis*, v. 37, no.8, p.1633-1656., DOI: [10.1007/BF01912193](https://doi.org/10.1007/BF01912193)
- Davidovits, J., 2002, 30 years of successes and failures in geopolymer applications. Market trends and potential breakthroughs. In *Geopolymer 2002 Conference*, Saint-Quentin, France.
- Dimas, D., Giannopoulou, I., and Panias, D., 2009, Polymerization in sodium silicate solutions: a fundamental process in geopolymerization technology: *Journal of Materials Science*, v.44, no.14, p. 3719-3730, DOI:10.1007/s10853-009-3497-5
- Frisch, H. L., 1980, Sorption and transport in glassy polymers-a review: *Journal Polymer Engineering and Science*, v.20, no.1, p. 2-13, DOI: 10.1002/pen.760200103
- Heah, C.Y., Kamarudin, H., Mustafa, A., Bakri, A.M., Bnhussain, M., Luqman, M., Khairul Nizar, I., Ruzaidi, C.M., and Liew, Y.M., 2012, Study on solids-to liquids and alkaline activator ratios on kaolin-based geopolymers: *Construction and Building Materials*, v.35, p.912-922.
- Huling, S.G., and Pivetz, B.E., 2006, In-Situ Chemical Oxidation: *Engineering Issue*, p.1-60, Report prepared for United States Environmental Protection Agency by the Office of Research and Development National Risk Management Research Laboratory Cincinnati, OH.
- Ibaraki, M., and Schwartz, F. W., 2001, Influence of natural heterogeneity on the efficiency of chemical floods in source zones: *Ground Water*, v.39, no.5, p.660-666.
- Khale, D., and Chuadhary, R., 2007, Mechanism of geopolymerization and factors influencing its development: A review: *Journal of Materials Science*, v.42, p.729-746.
- Kong, D.L.Y., Sanjayan, R., and Sagoe-Crentsil, K., 2007, Comparative performance of geopolymers made with metakaolin and fly ash after exposure to elevated temperatures: *Cement and Concrete Research*, v.42, p. 1583-1589.
- Lee, E.S., and Schwartz, F.W., 2007, Characterization and optimization of long-term controlled release system for groundwater remediation: A generalized modeling approach: *Chemosphere*, v.69, no.2, p.247-253, DOI:10.1016/j.chemosphere.2007.04.037
- Lee, E.S., Woo, N.C., Schwartz, F.W., Lee, B.S., and Lee, K.C., 2008, Characterization of controlled-release KMnO<sub>4</sub> (CRP) barrier system for groundwater remediation: A pilot-scale flow-tank study: *Chemosphere*, v.71, no.5, p.902-910, DOI:10.1016/j.chemosphere.2007.11.037.

- Li, X.D., and Schwartz, F.W., 2004, DNAPL mass transfer and permeability reduction during in situ chemical oxidation with permanganate: *Geophysical Research Letters*, v.31, no.6, DOI: 10.1029/2003GL019218
- Lizcano, M., Gonzalez, A., Basu, S., Lozano, K., Radovic, M., and Viehland, D., 2012, Effects of water content and chemical composition on structural properties of alkaline activated metakaolin-based geopolymers: *Journal of the American Ceramic Society*, v.95, no.7, p.2169-2177, DOI: 10.1111/j.1551-2916.2012.05184.x.
- Peppas, N.A., 1985, Analysis of Fickian and non-Fickian drug release from polymers: *Pharmaceutica Acta Helvetiae*, v.60, no.4, p.110-11.
- Ritger, P.L., and Peppas, N., 1987, A simple equation for description of solute release II. Fickian and anomalous release from swellable devices: *Journal of Controlled Release*, v.5, no.1, p.37-42, DOI:10.1016/0168-3659(87)90035-6
- Ross, C., Murdoch, L., Freedman, D., and Siegrist, R., 2005, Characteristics of Potassium Permanganate Encapsulated in Polymer: *Journal of Environmental Engineering*, v.131, no.8, p.1203-1211, DOI: 10.1061/(ASCE) 0733-9372.
- Rowles, M., and O'Conner, B., 2003, Chemical optimization of the compressive strength of aluminosilicate geopolymers synthesized by sodium silicate activation of metakaolinite: *Journal of Materials Chemistry*, v.13, no.5, p.1161-1165, DOI: 10.1039/B212629J
- Seipmann, J., Siegel, R.A., and Seipmann, F., 2012, Diffusion controlled drug delivery systems: *Fundamentals and Applications of Controlled Release Drug Delivery, Advances in Delivery Science and Technology*, p. 127-152. New York: Springer.
- Siegrist, R., Crimi, M., Simpkin, T.J., Borden, R.C., 2011, In Situ Chemical Oxidation for Groundwater Remediation: *SERDP ESTCP Environmental Remediation Technology*, v.3, p.1-60, DOI: 10.1007/978-1-4419-7826-4.
- Siegrist, R., Lowe, K.S., Lawrence, C.M., Case, T.L., and Pickering, D.A., 1999, In situ oxidation by fracture emplaced reactive solids: *Journal of Environmental Engineering*, v.125, no.5, and p.429-440.
- Solpuker, U., Cotter, Z., Kim, Y., and Schwartz, F.W., 2014, Potassium Permanganate Doped Geopolymers for Remedial Applications: *Groundwater Monitoring and Remediation*, v.34, no.4, p.93-101, DOI: 10.1111/gwmr.12087
- Yan, E., and Schwartz, F. W., 1999, Oxidative degradation and kinetics of chlorinated ethylenes by potassium permanganate: *Journal of Contaminant Hydrogeology*, v.37, no.3-4, p.343-365, DOI:10.1016/S0169-7722(98)00166-1
- Yuan, B., Fei, L., Yanmei, C., and Ming-Lai, F., 2013, :*Journal of Environmental Sciences*, v.25, no.5, p.971-977. DOI:10.1016/S1001-0742(12)60134-X
- Zhang, H., and Schwartz, F.W., 2000, Simulating the in situ oxidative treatment of chlorinated ethylenes by potassium permanganate: *Journal of Water Sources Research*, v.36, no.10, p.3031-3042.

## APPENDIX

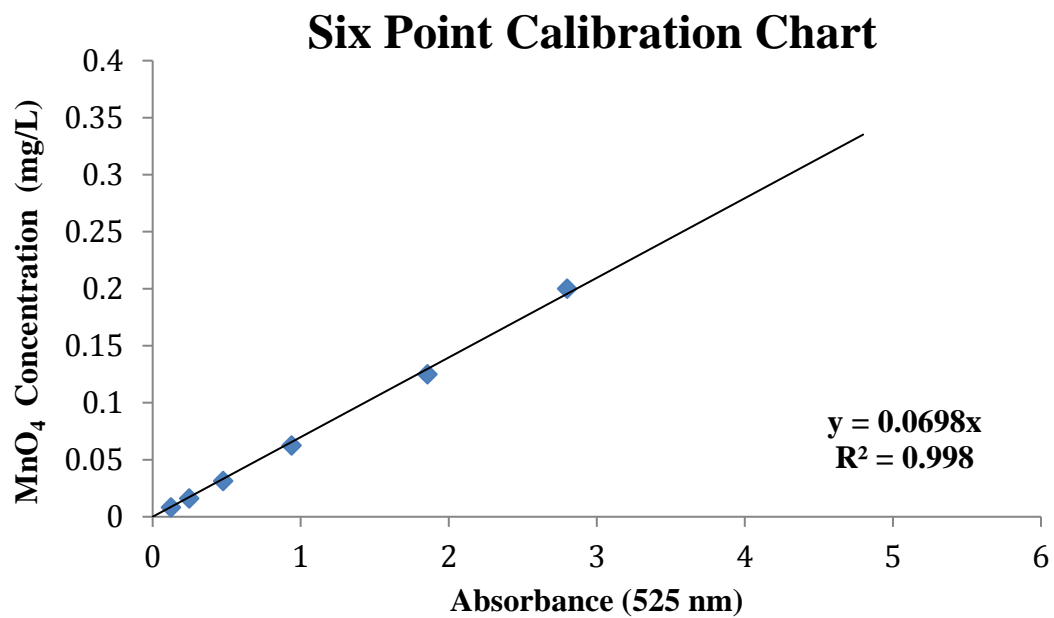


Figure A1. Six point calibration chart used to calculate permanganate concentration from absorbance.